Songklanakarin J. Sci. Technol.
36 (4), 471-475, Jul. - Aug. 2014

SJST SONGKLANAKARIN JOURNAL OF SCIENCE AND TECHNOLOGY
http://www.sjst.psu.ac.th

Original Article

Investigation of entrance length in circular and noncircular conduits by computational fluid dynamics simulation

Pimpun Tongpun, Eakarach Bumrungthaichaichan, and Santi Wattananusorn*

School of Chemical Engineering, Faculty of Engineering,
King Mongkut's Institute of Technology Ladkrabang, Lat Krabang, Bangkok, 10520 Thailand.

Received 28 November 2013; Accepted 21 March 2014

Abstract

This study estimated entrance length of circular and noncircular conduits, including circle, triangle, square and hexagon cross-sectional conduit, by using computational fluid dynamics (CFD). For simulation condition, the length of non-circular conduit was 10 m and the hydraulic diameter was 0.2 m. The laminar flow with Reynolds number of 500 and turbulent flow with Reynolds number of 50,000 were applied to investigate water flow in conduits. The governing equations were solved iteratively by using ANSYS FLUENT 14.0. For turbulent flow simulation, standard k-epsilon and RNG k-epsilon model were employed to simulate turbulence. The preliminary results were validated by comparison with theoretical data. At first, grid independency was evaluated to optimize the model. Norm* was employed to investigate the entrance length, which is related to velocity. The simulated results revealed that the entrance length for laminar flow was longer than turbulent flow.

Keywords: CFD, entrance length, noncircular

1. Introduction

Process parameters such as flow rate, temperature, pressure, pH, and others are important for the quality control and production management in any factory. The accurate prediction of flow measurement in a conduit is important in many industries. Therefore, the installation position of a flow meter is of great importance when accurate flow measurements are required. The position of a measurement and the performance of a device are required to achieve accurate process parameters for high performance production planning. The position of a measurement should be set-up when the flow rate is constant after an entrance length zone. The entrance length is affected by many parameters, such as fluid type, conduit material, roughness, cross-sectional area, angle at the corner of conduit, etc. Usually, noncircular conduits were employed for relative small pressure drop system, especially in the heating and cooling system. The fluid flow behavior is different because of the friction factor of different cross-sectional areas (Morrison, 2013).

Generally, the fluid flow in a conduit can be distinguished into two zones, including developing zone (entrance zone) and fully developed zone. In the developing zone, the boundary layer is not fully developed. Therefore, the velocity profile changes along the longitudinal distance. The boundary layer grows downstream until the inviscid core disappears. So, the velocity profile no longer changes with increasing the distance downstream. This region is called fully developed zone. In order to obtain the accurate parameters, the measuring device should be installed in the fully developed zone.

The length between conduit inlet and fully developed zone can be determined by using the entrance length (L_h). The entrance length of laminar flow and turbulent flow can be approximated by using the correlations in Equation 1 and 2, respectively; see Ye *et al.* (2006) and Ngo and Gramoll (2013).

* Corresponding author.
Email address: santi_wattananusorn@hotmail.com

$$\frac{L_h}{D} \approx 0.06\,\mathrm{Re} \tag{1}$$

$$\frac{L_h}{D} \approx 4.4(\mathrm{Re})^{1/6} \tag{2}$$

where D is conduit diameter. For noncircular conduits, the hydraulic diameter can be used instead of the conduit diameter and can be calculated by equation as expressed in Table 1.

There have been a number of studies concerned with noncircular conduits. Most of these studies culminate in pressure drop and entrance length in noncircular conduit. Hetsroni *et al.* (2005) considered fluid flow in micro-channels, including circular, rectangle, triangular and trapezoidal micro-channels with hydrodynamic diameters in the range of 1.01 to 4010 μm. The results showed that the viscous energy affected by the relation of hydrodynamic diameter to channel length and Reynolds number. For a Reynolds number less than the critical Reynolds number, an oscillatory regime might occur in a micro channel. Tamayol and Bahrami (2010) investigated laminar flow in micro channels with noncircular cross section, including circle, ellipse, rectangle, rectangle-with-round-corners, rhombus, star-shape, equilateral triangle, square, pentagon, and hexagon. They successfully predicted velocity distribution and pressure drop and the data compared with experimental results from other studies. Durst *et al.* (2005) employed numerical, experimental and analytical methods to study the development lengths of laminar pipe and channel flows. They numerically studied and proposed a linear relationship between entrance length and Reynolds number as $X_D/D = [0.619^{1.6} + (0.0567\mathrm{Re})^{1.6}]^{1/1.6}$. Muzychka *et al.* (2009) employed scale analysis and modeling approach to develop a simple model of pressure drop in laminar developing flow which only requires two parameters, including the aspect ratio of the duct and the dimensionless duct length.

For turbulent flow, Bhandari and Singh (2012) employed computational fluid dynamics (CFD) technique to determine the turbulent flow in pipe. They analyzed velocity and skin friction coefficient along the pipe length with two different fluids, air and water. The simulated results were in good agreement with analytical method. The results revealed that skin friction coefficient and axial velocity decreased and increased with the pipe length, respectively. Duan *et al.* (2012) investigated the pressure drop for fully developed turbulent flow in noncircular channels with normal conditions of engineering practice. Their proposed models gave the accuracy of 6% for most common duct shapes and can be used to predict the pressure drop of fully developed turbulent flow in noncircular ducts.

Noncircular conduits usually applied to heat exchangers and reactors, which are used in the chemical engineering. Thus, the aim of the present study is to predict the entrance length of noncircular conduits, including triangle, square and hexagon cross-sectional shape, by using the CFD technique. The Navier-Stokes equations for steady state flow were employed to simulate laminar flow in pipe. For turbulent flow, the standard k-epsilon and RNG k-epsilon turbulence model were adopted to achieve fluid flow field.

2. Governing equations

The models were three-dimensional steady flow with constant kinematic viscosity. The system was governed by continuity equation, momentum equations and k-epsilon turbulence model.

The time average equations for steady incompressible of continuity equation and momentum equation can be written in the following form.

Continuity equation:

$$\nabla \cdot \overline{\mathbf{V}} = 0 \tag{3}$$

Momentum equation

$$\nabla \cdot \left(\rho \overline{\mathbf{V}}\overline{\mathbf{V}}\right) = -\nabla p + \nabla \boldsymbol{\tau} + S_M \tag{4}$$

where $\overline{\mathbf{V}} = \overline{u}\,\mathbf{i} + \overline{v}\,\mathbf{j} + \overline{w}\,\mathbf{k}$

For turbulent flow, k-epsilon model was adopted to simulate the turbulence. The k-epsilon model is one of the most common turbulence models which includes two extra transport equations to represent the turbulent properties of the flow. The first equation is transport equation of turbulent kinetic energy (k) and the second one is transport equation of dissipation rate of turbulent kinetic energy (ε). The general form of these equations can be written as the follows.
k-transport equation:

$$\frac{\partial}{\partial t}(\rho k) + \frac{\partial}{\partial x_i}(\rho k \overline{u_i}) = \frac{\partial}{\partial x_j}\left[\left(\mu + \frac{\mu_t}{\sigma_k}\right)\frac{\partial k}{\partial x_j}\right] + G_k + G_b - \rho\varepsilon - Y_M + S_k \tag{5}$$

ε - transport equation

$$\frac{\partial}{\partial t}(\rho \varepsilon) + \frac{\partial}{\partial x_i}(\rho \varepsilon \overline{u_i}) = \frac{\partial}{\partial x_j}\left[\left(\mu + \frac{\mu_t}{\sigma_\varepsilon}\right)\frac{\partial \varepsilon}{\partial x_j}\right] + C_{l\varepsilon}\frac{\varepsilon}{k}(G_k + C_{3\varepsilon}G_b) - C_{2\varepsilon}\rho\frac{\varepsilon^2}{k} + S_\varepsilon \tag{6}$$

where

$$\mu_t = \rho C_\mu \frac{k^2}{\varepsilon},\ G_k = -\rho\overline{u_i' u_j'}\frac{\partial \overline{u_j}}{\partial x_i},\ G_b = \beta g_i \frac{\mu_t}{\mathrm{Pr}_t}\frac{\partial T}{\partial x_i},$$

$$Y_M = 2\rho\varepsilon M_t^2,\ C_{3\varepsilon} = \tanh\left|\frac{v}{u}\right|,\ \sigma_k = 1.0,\ \sigma_\varepsilon = 1.3,$$

$$C_{1\varepsilon} = 1.44,\ C_{2\varepsilon} = 1.92, \text{ and } C_\mu = 0.09$$

3. Numerical Method

The model was a noncircular conduit. The length and hydraulic diameter of noncircular conduit were 10 m and 0.2 m, respectively. The three-dimensional models were done by GAMBIT. The water density and viscosity were 998.2 kg/m^3 and 0.001003 kg/(m·s), respectively. The water inlet was assumed to be uniform flow. The fluid velocity for laminar flow and turbulent flow were 0.0025 m/s (Re = 500) and 0.251 m/s (Re = 50,000), respectively. At the wall, no-slip boundary condition was applied. For turbulent flow, standard k-epsilon and RNG k-epsilon model were employed to simulate the turbulence.

Governing equations were solved numerically by using ANSYS FLUENT 14.0. The pressure-velocity coupling was solved by using SIMPLE algorithm. The numerical scheme for pressure, momentum was standard and second order upwind, respectively. The interpolation scheme of turbulence quantities were first order upwind.

Extensive grid refinement tests have been done on the flow fields of noncircular conduit to obtain grid independent solution. The cross-sectional mesh of this model is depicted in Table 1. The numerical solution was carried out with the residuals less than 10^{-4}.

4. Results and Discussion

4.1 Effect of grid generation on fluid flow behavior

The accurate of simulated results depends on many parameters, such as grid generation, interpolation scheme, etc. In order to obtain the grid independent solution, the near wall grid with different grid numbers, including 10, 12, 14 and 16, were employed to simulate the water flow in circular conduit with a Reynolds number of 500. The simulated centerline axial velocity profile of these models are shown in Figure 1. The dimensionless velocity, which is defined as the ratio of centerline axial velocity to inlet velocity (V/V_{inlet}), at the end of conduit of these 4 different models were expressed in Table 2. The error of these cases were less than 1% when comparing with the predicted dimensionless velocity obtained by the model with 10 near wall grids. According to these results, it has been observed that the model with 10 near wall grids provides a sufficient grid independency. However, for excluding any uncertainty, computations have been performed by using the model with 14 near wall grids.

4.2 Effect of hydraulic diameter of triangle on entrance length

This research studied the effect of hydraulic diameter of triangle on entrance length. The triangle geometries of this study and their entrance lengths are shown in Table 3. In this study, the entrance length was determined by using Norm*. The Norm* can be expressed as shown in equation (7).

$$Norm^* = Norm / V_{inlet} \quad (7)$$

where $Norm = \left(\sum_{i=1}^{N} \left(V_i - \tilde{V}_i \right)^2 \right)^{1/2}$, V_i and $\tilde{V}_i$ are the mean velocities along the flow direction (or 2-direction) at the same position of the adjacent cross section (or xy-plane).

The simulated Norm* along the longitudinal distance of these 3 different triangle geometries are shown in Figure 2. In this figure, it can be seen that the fluid flow of these model are similar. Moreover, the entrance length of the triangle with the base length of 0.5 m showed the highest value because of the smaller angle corner.

Table 1. Conduit geometries and their hydraulic diameters.

Geometry	Shape	D_h
Circle	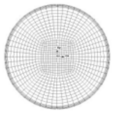	$2r$
Triangle	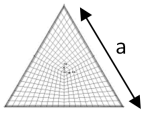	$\frac{\sqrt{3}a}{3}$
Square	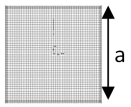	a
Hexagon	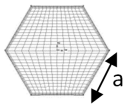	$\frac{a}{\tan\left(\frac{\pi}{6}\right)}$

Table 2. Dimensionless velocity at the end of conduit.

Number of near wall grid	V/V_{inlet}	%Error
10 (IC10)	1.988	0.00
12 (IC12)	1.991	0.14
14 (IC14)	1.992	0.22
16 (IC16)	1.993	0.27

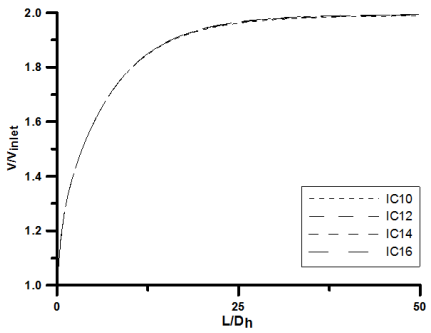

Figure 1. The centerline velocity profile for different near wall grid generations.

Table 3. Details of 3 different triangle cross-sectional conduits and their entrance lengths.

Parameter	Base Length (m)	High (m)	D_h (m)	L/D_h
Triangle1	0.346	0.300	0.200	28.1
Triangle2	0.500	0.300	0.234	42.1
Triangle3	0.200	0.300	0.144	33.0

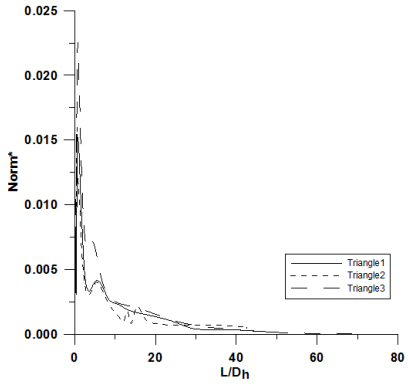

Figure 2. The Norm* of 3 different triangle cross-sectional conduits.

4.3 Effects of noncircular conduits and Reynolds number on entrance length

The Norm* of different conduits and Reynolds numbers are shown in Figure 3. In Figure 3, it can be seen that the Norm* value at the entrance zone exhibited a large deviation due to unsteady behavior, then decrease and approach to zero value. Moreover, the velocity profiles of circle and square conduits exhibited similar behavior. These results were in good agreement with numerical results reported by F. Anselmet (2009). Norm* of laminar flow illustrated high deviation for 4 different cross-sectional areas. While Norm* of turbulent flow represented lower deviation, which indicates the shorter fully developed length. Norm* results obtained by RNG k-epsilon model represented smooth curve and low deviation because the swirl flow correction is added to RNG k-epsilon model, see RNG k-epsilon model (2014).

According to fluid flow simulations, the entrance length of 4 different conduits were expressed in the Table 4. It can be seen that the triangle cross-sectional conduit showed the shortest entrance length in laminar flow. This might be caused by higher energy loss by wall friction and higher interference at the corner (Wattananusorn, 2004). In turbulent flow simulation, the RNG k-epsilon model showed the shorter entrance length of when comparing with the results obtained by standard k-epsilon model.

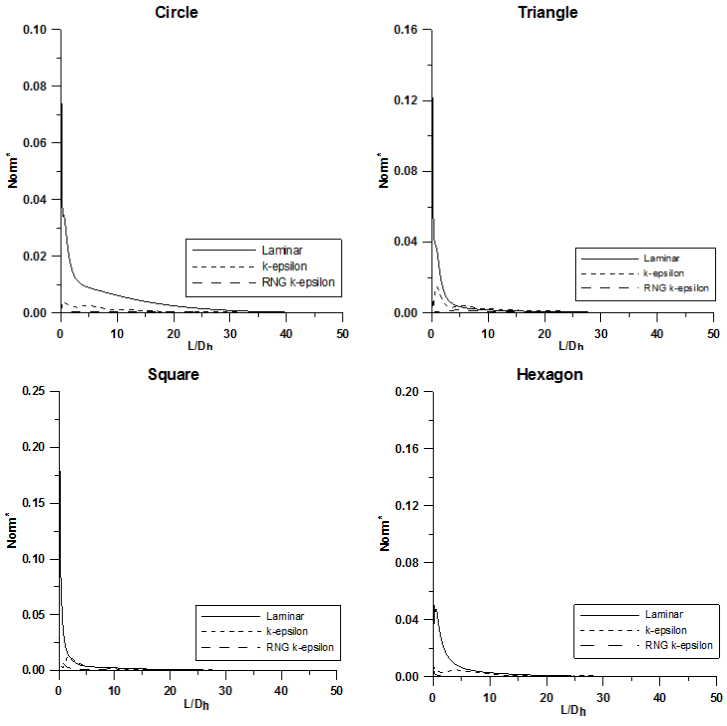

Figure 3. The Norm* of 4 different noncircular conduits.

Table 4. Entrance length of noncircular conduits at Norm* of 9.58×10^{-4} for laminar flow and 5.35×10^{-4} for turbulent flow.

Cross-sectional shape	L/D_h		
	Laminar flow	Turbulent flow (k-epsilon)	Turbulent flow (RNG k-epsilon)
Circle	30.0	26.7	2.3
Triangle	18.5	28.1	17.0
Square	22.5	28.7	12.7
Hexagon	21.0	19.1	24.0

5. Conclusions

CFD simulation has been employed to investigate the fully developed length of laminar and turbulent flow in circular and noncircular conduits. According to gird independent study, the model with 14 near wall grids was selected to simulate the fluid flow behavior. Laminar flow represented longer entrance length when comparing with turbulent flow. In contrast, the laminar flow of triangle cross-sectional conduit exhibited the shorter entrance length. The simulated entrance lengths obtained by RNG k-epsilon model were shorter than the results simulated by standard k-epsilon model except hexagon cross-sectional conduit.

References

Anselmet, F., Ternat, F., Amielh, M., Boiron, O., Boyer, P., and Pietri, L. 2009. Axial development of the mean flow in the entrance length region of turbulent pipe and duct flows. C. R. Mecanique. 337, 573-584.

Bhandari, D. and Singh, S. 2012. Analysis of fully developed turbulent flow in a pipe using computational fluid dynamics. International Journal of Engineering Reasearch and Technology. 1, 1-9.

Duan, Z., Yovanovich, M.M. and Muzychka, Y.S. 2012. Pressure drop for fully developed turbulent flow in circular and noncircular ducts. Journal of Fluids Engineering. 134, 061201-1-10.

Durst, F., Ray, S., Unsal, B. and Bayoumi, O.A. 2005. The development lengths of laminar pipe and channel flows. Journal of Fluids Engineering. 127, 1154-1160.

Faghani, E., Saemi, S., Maddahian, R. and Farhanieh, B. 2009. Numerical investigation of corner angle and wing number effects on fluid flow characteristics of a turbulent stellar jet. Heat Mass Transfer. 46, 25-37.

Gerhart, P.M., Gross, R.J. and Hochstein J.I. 1992. Fundamentals of Fluid Mechanics, Addison-Wesley Pub. Co., U.S.A.

Hetsroni, G., Mosyak, A., Pogrebnyak, E. and Yarin, L.P. 2005. Fluid flow in micro-channels. International Journal of Heat and Mass Transfer. 48, 1982-1998.

Morrison, F.A. 2013. An introduction to fluid mechanics, Cambridge University Press, UK.

Muzychka, Y.S. and Yovanovich, M.M. 2009. Pressure drop in laminar developing flow in noncircular ducts: A scaling and modeling approach. 131, 111105-1-11.

Ngo, C.C. and Gramoll, K. Fluid Mechanics Theory. https://ecourses.ou.edu/cgi- bin/eBook.cgi?doc=&topic=fl&chap_sec=08.3&page=theory [October 10, 2013]

RNG k-epsilon model. http://www.arc.vt.edu/ansys_help/flu_th/flu_th_sec_turb_rng. html#flu_th_eq_rng_diff_visc [February 2, 2014]

Tamayol, A. and Bahrami, M. 2010. Laminar flow in microchannels with noncircular cross section. Journal of Fluids Engineering. 132, 111201-1-9.

Wattananusorn, S. 2004. Interference of laminar flow on displacement thickness in a streamwise corner. Journal of Power and Energy. 218, 51-53.

Ye, Q., Kim, Y. and Steudle, E. 2006. A re-examination of the minor role of unstirred layers during the measurement of transport coefficients of Chara coralline internodes with the cell pressure probe. 29, 964-980.